



TM-912  
2529.000  
October 1979

CONSTRUCTION AND OPERATION OF AN ELECTROMAGNETIC SHOWER DETECTOR

P. H. Garbincius and V. A. Polychronakos  
Fermilab, Batavia, Illinois 60510

D. S. Barton, T. Dobrowolski, C. Halliwell,  
H. W. Kendall, T. Lyons, and C. C. Young,  
Massachusetts Institute of Technology,  
Cambridge, Massachusetts 02139

J. Nassalski and T. Siemiarczuk  
Institute of Nuclear Research, Warsaw, Poland

ABSTRACT

An electromagnetic shower detector consisting of lead glass blocks and scintillator hodoscopes was constructed. During calibration runs detector resolutions were measured for single incident electrons. Performance of the detector for  $\pi^0$  and multi-photon showers, including sizable backgrounds, was studied during actual data runs. This detector was used in Fermilab Experiment 451.

FOR PRESENTATION  
at the

IEEE 1979  
Nuclear Science Symposium  
October 17-19, 1979  
San Francisco, California

# CONSTRUCTION AND OPERATION OF AN ELECTROMAGNETIC SHOWER DETECTOR

P. H. Garbincius and V. A. Polychronakos<sup>(a)</sup>  
Fermilab\*, Batavia, Illinois 60510

D. S. Barton,<sup>(a)</sup> T. Dobrowolski,<sup>(b)</sup> C. Halliwell,<sup>(c)</sup>  
H. W. Kendall, T. Lyons, and C. C. Young,<sup>(d)</sup>  
Massachusetts Institute of Technology,  
Cambridge, Massachusetts 02139

J. Nassalski and T. Siemiarczuk  
Institute of Nuclear Research, Warsaw, Poland

## ABSTRACT

An electromagnetic shower detector consisting of lead glass blocks and scintillator hodoscopes was constructed. During calibration runs detector resolutions were measured for single incident electrons. Performance of the detector for  $\pi^0$  and multi-photon showers, including sizable backgrounds, was studied during actual data runs.

## INTRODUCTION AND DESCRIPTION

An electromagnetic shower detector was built for Fermilab Experiment 451 to study high transverse momentum processes in hadron-nucleus collisions. This apparatus detected high  $P_t$  ( $> 1.5$  GeV/c)  $\pi^0$  and multi-photon events and triggered a vertex detector<sup>1</sup> to study the dependence of recoil jet properties on the atomic number of the target.

The detector is schematically shown in Figures 1 and 2. Shower energy was measured with lead glass blocks. Positional information was determined by pulse height analysis of X-Y scintillator hodoscopes placed at shower maximum. A novel wedge-shaped scintillation counter formed a simple analog  $P_t$  signal which provided a data trigger. A combination of hydrogen thyratron and radioactive sources was used to monitor the individual photomultiplier gains. The detector subtended 15 mill-steradians, and was positioned at approximately 90 degrees in the center of mass reference frame.

The detector is somewhat similar to that described by M. Heller et al<sup>2</sup>. However we will discuss

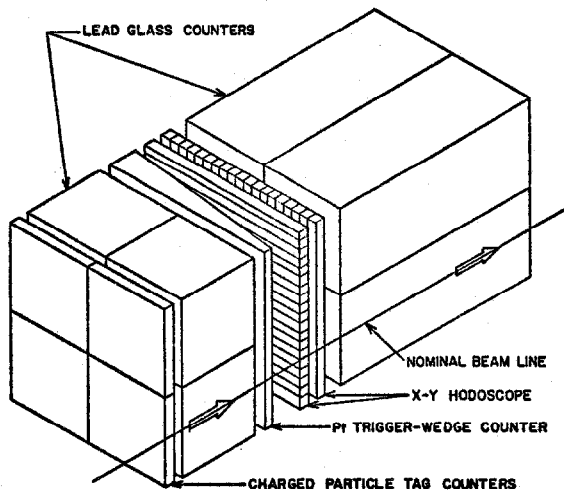


Fig. 1.  $\pi^0$  Detector Components.

\*Operated by Universities Research Association, Inc.  
Under Contract with U. S. Department of Energy.

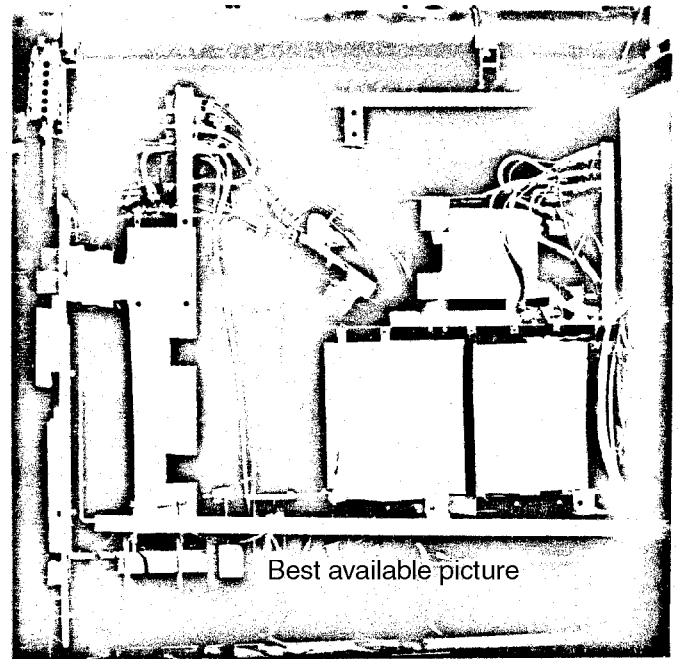


Fig. 2. Assembled  $\pi^0$  Detector.

not only test beam data, but also performance in an experimental data run during the summer of 1978.

## CONSTRUCTION DETAILS

We desired to detect high  $P_t$  single particles in order to study the associated charged particles produced in large transverse momentum processes. An electromagnetic shower detector allowed identification and measurement of high  $P_t$   $\pi^0$ 's and gamma rays within severe space constraints. Typical beam intensities were  $2 \times 10^6$  hadrons/sec incident on targets of 5% of an interaction length. This translated into a range of  $1.5 \leq P_t \leq 4$  GeV/c observable with reasonable statistics. Incident beam momentum of 100 GeV/c indicated a detected  $\pi^0$  momentum range of 10-40 GeV/c for the detector centered at 90° in the center of mass. The face of the detector was only 80 inches from the target, indicating that most  $\gamma$ 's from the  $\pi^0$  decay would coalesce and appear as a single electromagnetic shower.

### Lead Glass Counters

The shower energy was measured in 8 blocks of SF5 lead glass. There were 4 identical modules each consisting of two blocks, the pre-radiator and the radiator. The total depth was 22.6 radiation lengths, enough to contain a 40 GeV electromagnetic shower. The pre-radiator was 6.4 radiation lengths deep to allow the insertion of the position hodoscopes and the wedge

TABLE I. COUNTER PARAMETERS

NAME	NUMBER	DIMENSIONS	MATERIAL	PHOTOTUBE
Tag	4	6" h x 8" v x 1/2" t	Scintillator	6342A
Pre-radiator	4	6" h x 8" v x 6" t	Souvirel SF5 Lead Glass	4525
Wedge- $P_t$ Trigger	1	12" h x 12" v x (1/4"-1") t	Scintillator	56AVP
Vertical Position Slats	19	12" h x 0.63" v x 1/4" t	Scintillator	931A
Horizontal Position Slats	19	0.63" h x 12" v x 1/4" t	Scintillator	931A
Radiator	4	5 3/4" x 5 3/4" x 15"	Ohara SF5 Lead Glass	4525
Reference	2	-	Bi <sup>207</sup> + Scintillator	6342A

trigger counter. This depth was chosen<sup>3</sup> such that the average shower density is approximately proportional to shower energy over the operated  $\gamma$ -energy range.

The pre-radiator phototubes were mounted vertically, transverse to the shower, while the radiator phototubes were mounted on the downstream end. The RCA 4525 phototube was used along with a simple resistor divider base providing typical divider currents of about 1 mAmp. The relatively slow 150 nsec pulse width of the lead glass and the 4525 did not present serious pile-up problems at normal data rates.

Wratten 2A filters were installed between the lead glass and the phototubes to improve resolution by making the response less dependent on geometric position or longitudinal shower fluctuations.<sup>4</sup> Optical grease and spring tension coupled the phototube to the lead glass. The four counters in both the pre-radiator and radiator sections were each wrapped in aluminized mylar for optical isolation and were contained within a light-tight aluminum box. An additional iron box around the phototubes provided magnetic shielding.

#### Position Hodoscopes and Charged Particle Tag Counters

The position of the electromagnetic shower was determined using crossed X-Y scintillator slats positioned near shower maximum. There were 19 scintillation counters of transverse size 0.63 inches (1.6 cm) in each plane. Lucite rod light pipes coupled the counters to the RCA 931A phototubes. The shower position determination used the hodoscope pulse heights which sampled the transverse size of the shower. The hodoscope signals were integrated in 8-bit, ADC's using 60 nsec gates. Four simple scintillation counters were installed upstream of the pre-radiator to tag events with extra charged particles incident upon the detector.

#### Wedge Trigger Counter

Various schemes<sup>5</sup> have been devised for generating a  $P_t$  trigger for complicated calorimetric devices.

These triggers required delicate on-line gain balancing and continuous calibration of many phototubes to insure consistent operation. We attempted to simplify operations by placing a single scintillation counter downstream of the pre-radiator near shower maximum. This counter was machined into a wedge shape such that the scintillator thickness was proportional to the distance from the nominal beam line. The signal in this counter was proportional to the number of shower particles (proportional to the shower energy) times the distance from the beam line (production angle), thereby forming  $P_t$  directly.

The scintillator was mounted to a lucite light pipe. In addition, all planar surfaces were covered by BBQ-lightbars, then wrapped with aluminum foil. This gave reasonable light collection uniformity over the face of the wedge. The counter was coupled to a 56 AVP phototube with a transistorized high rate base. The coincidence of a minimum pulse height in the

wedge counter and a valid beam particle signaled a high  $P_t$  electromagnetic event candidate and triggered the data acquisition system.

#### Calibration and Gain Tracking

The entire detector was mounted on a remotely moveable cart and swept both horizontally and vertically across a known incident beam. Using a 30 GeV  $e^+$  beam, the calibration constants (ADC pedestals and GeV per channel gains) for the lead glass and hodoscope counters were measured at the beginning of the data run.

Detector gain drifts were monitored during special runs over the one month data cycle using a self-calibrating light flasher system. Two RCA 3C45 hydrogen thyratron light sources<sup>6</sup> were alternately pulsed producing light flashes of about 30 nsec duration. The thyratron light was directed to each counter, opposite to the photomultiplier, using glass fiber optics light guides. These pulses were also directed to two special reference tubes each outfitted with Bi<sup>207</sup> doped scintillators. The reference tube #1 pedestal was measured by triggering on the reference #2 Bi<sup>207</sup> source. The reference tube absolute gain was determined by fitting the 1 MeV Bi<sup>207</sup> conversion electron spectrum. The two thyratron flasher pulses were then measured by the reference tubes giving an absolute measure of their light outputs. These known thyratron signals were then compared with their signals in the lead glass and hodoscopes, thereby determining the gain of each counter. Gain corrections were then added in the later data analysis programs.<sup>7</sup> The average thyratron light flashes in the lead glass counters approximated the light produced by 10 GeV electron showers.

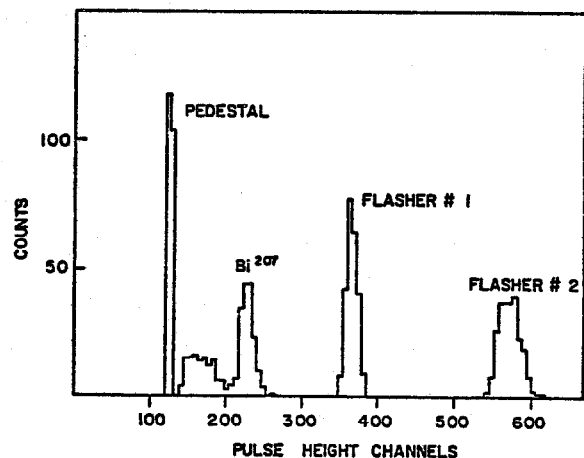


Fig. 3. Reference Counter Calibration Pulse Height Spectrum.

## CALIBRATION RESULTS

Preliminary testing used tagged electrons of 5-30 GeV/c momenta. Actual calibration occurred just before data taking using 30 GeV/c Cerenkov tagged positrons. The beam phase space was described by

$$\sigma_h = \sigma_v = 1.7 \text{ mm}, \sigma_p/p = 0.1\%$$

### Lead Glass Counters

Each lead glass module in turn was centered on the beamline. After rough determination of the pedestal and gain constants, a least-squares fit<sup>8</sup> found calibration constants to optimize the energy resolution of each pre-radiator plus radiator module. The average resolution was  $\sigma_E/E = 1.9\%$  or  $\text{FWHM}/E = 4.5\%$ .

Two other similar lead glass detector resolutions at 30 GeV were:

$$\text{FWHM}/E = 3.3\% \text{ (Ref.8) and } \text{FWHM}/E = 4.9\% \text{ (Ref.2)}$$

The data showed good energy linearity to better than 6% over the range 10-30 GeV. The typical lead glass energy deposited by 30 GeV/c hadrons was measured to be 0.5 GeV.

Strong correlations between the pre-radiator and radiator energy depositions are shown in Fig. 4. The considerably sharper resolution of the sum shows the effects of fluctuations of the longitudinal shower development.

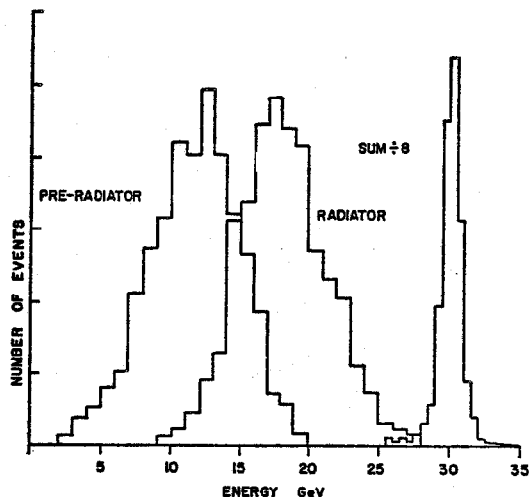


Fig. 4. Typical 30 GeV energy distribution curves for pre-radiator, radiator and total energy sum.

A horizontal scan of the detector across the beam (Fig. 5) showed the spatial uniformities of the individual elements along with that of the composite detector. The 5% rise in the total observed energy near the G1-G4 boundary indicated a slight increase in light collection efficiency near the lead glass counter edges.

### Hodoscopes

The average shower position at 30 GeV, obtained by weighting the hodoscope slat position by its pulse height, produced a reconstructed position resolution  $\sigma = 2.5 \text{ mm}$ . This was comparable to that obtained by reference 2 using a shower maximum hodoscope and by reference 5 where the shower was longitudinally integrated for each slat. Note that this resolution was a factor of 6 smaller than the slat sampling size. The transverse shower distribution at a depth of  $6.4 X_0$

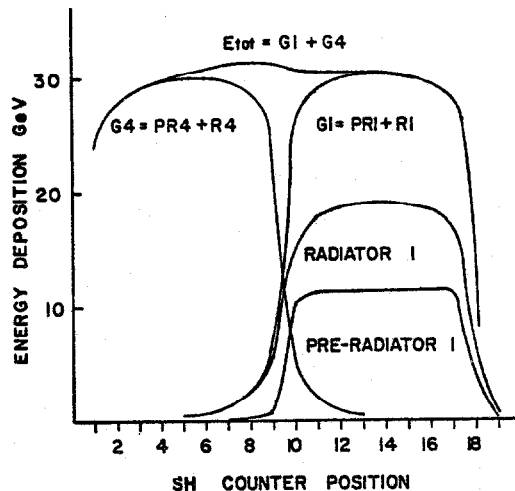


Fig. 5. Position response of the lead glass counters. Each SH counter is 1.6 cm wide.

can be parameterized as

$$\frac{dN}{dt} \sim e^{-|t|/a} \text{ where } a = 2.7 \text{ cm at } 30 \text{ GeV.}$$

The distance between the pre-radiator and hodoscopes was 3.5 inches. The reconstructed position was linear in the incident beam position except near the detector edges where the deviations from linearity were due to the finite transverse integration of the shower distribution, and were easily correctable.

### $P_t$ Resolution

The reconstructed  $P_t$  of each shower was determined by the lead glass energy and the X-Y hodoscope positions. As measured by position sweeps, the reconstructed  $P_t$  had a resolution of

$$\sigma_{P_t} = 0.1 \text{ GeV/c at } 30 \text{ GeV energy,}$$

independent of position.

### Wedge Counter

The response of the wedge counter to 30 GeV positrons is shown in Fig. 6, showing that the horizontal response is indeed linear with the distance from the nominal beam line. The corresponding vertical scan shows a relative signal attenuation of 20% across the scintillator. The wedge energy resolution was  $\sigma_w/W = 14\%$  at 30 GeV, roughly independent of position. This indicated that we were limited in resolution by shower statistics.

## DATA TRIGGER STUDIES

The wedge counter provided a fast data trigger such that the trigger rate was approximately exponential in discriminator threshold setting. Typically, this threshold was set at  $P_t = 1.6 \text{ GeV/c}$ . The  $P_t$  reconstructed using the lead glass and hodoscopes could be described by a gaussian shape with peak  $\approx$  threshold and  $\sigma = 0.5 \text{ GeV/c}$ . Extrapolating the reconstructed distrib-

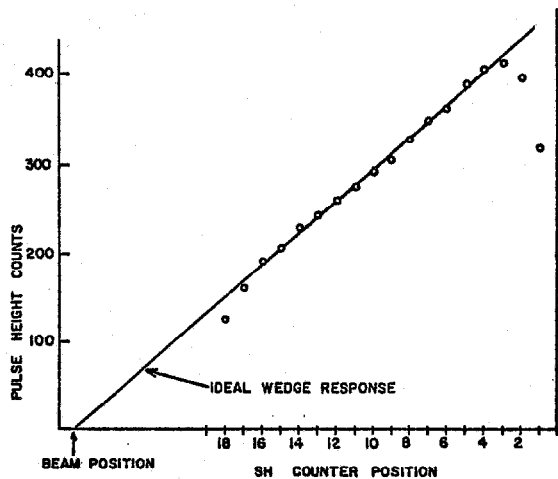


Fig. 6. Position response of the wedge counter. Each SH counter is 1.6 cm wide.

tion to low  $P_t$ , we found that the wedge counter trigger efficiency was 50% at the distribution peak,  $P_t = 1.6$ , and increased to 80% at  $P_t = 1.8$  GeV/c. This indicated that approximately 20% of the total triggers, those above 1.8 GeV/c, were relatively unbiased, and therefore directly useful for cross section analysis.

For data triggers, the average charged particle multiplicity incident upon the detector plane was 2.7 per trigger, as measured by the vertex detector proportional chambers. Similarly, even when triggers accompanied by charged particles were vetoed using the tag counters, a large multi-photon background remained. This background showed up as a large number of low energy showers in the hodoscopes and also in a flat distribution in the Peak Module Energy/Total Lead Glass Energy ratio in contrast to the sharply peaked distributions expected for single energetic  $\pi^0$  showers.<sup>5</sup> This indicated that the large  $P_t$  detected was composed of a number of relatively lower  $P_t$  particles correlated in jet-like events. The short distance, 2 meters, between target and detector precluded separating the two gamma rays from  $\pi^0$  decay during normal data running. Special runs with much reduced  $P_t$  trigger thresholds resolved the decay and

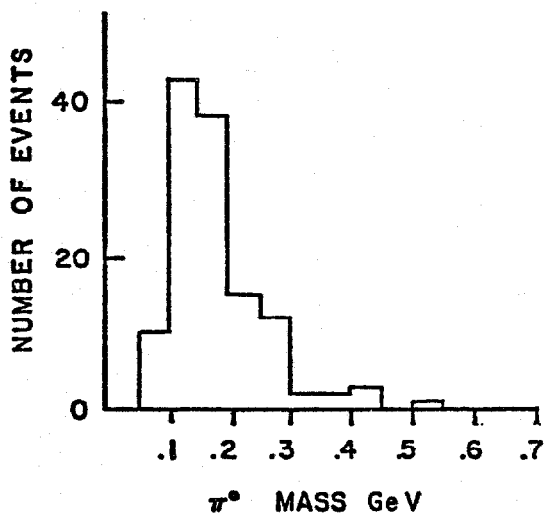


Fig. 7.  $\pi^0$  Mass spectrum for  $E_{\gamma\gamma} > 3$  GeV with no associated charged particles.

provided a  $\pi^0$  mass peak in Fig. 7.

#### CONCLUSION

This type of electromagnetic detector works well for single photons or electrons. Keeping the detector close to the target trades position resolution for increased solid angle. However, coincident, jet-like backgrounds are bothersome if the intention is the identification and measurement of multi-gamma states.

This wedge counter provides a quite adequate and very simple  $P_t$  trigger.

#### ACKNOWLEDGEMENT

We would like to thank the following people who also greatly contributed to this project: C. Kerns, R. Miksa, T. Minto, and H. Vaid of Fermilab, and M. Jacobs, and R. Strong of MIT. The work was supported in part by the U. S. Department of Energy and the National Science Foundation Special Foreign Currency Program.

#### REFERENCES

- (a) Present address: Brookhaven National Laboratory, Upton, N. Y. 11973.
- (b) Present address: CEN, Saclay, Gif-Sur-Yvette, France.
- (c) Present address: University of Illinois at Chicago Circle, Chicago, Illinois 60680.
- (d) Present address: Stanford Linear Accelerator, Stanford, California 94305.
- <sup>1</sup>L. Votta, Ph.D Thesis, M.I.T., 1979 (unpublished).
- <sup>2</sup>M. Heller, et al., Nucl. Instr. and Meth. 152 (1978) 379.
- <sup>3</sup>B. Rossi and K. Greisen, Rev. Mod. Phys. 13, 249 (1941).
- <sup>4</sup>R. J. Morrison, et al., Nucl. Instr. and Meth. 143 (1977) 311.
- <sup>5</sup>G. Donaldson, et al., Phys. Rev. Lett. 36, 1110, (1976),  
R. A. Johnson, Ph. D. Thesis, LBL-4610, 1975, and  
A. Ogawa, Ph.D. Thesis, LBL-8305, 1978.
- <sup>6</sup>J. Nagy and M. Binkley of Fermilab Experiment 95 provided the thyatron pulsing circuitry.
- <sup>7</sup>Similar gain tracking algorithms are described by R. Madaras, et al., Nucl. Instr. and Meth. 160, (1979) 263.
- <sup>8</sup>J. Appel, et al., Nucl. Instr. and Meth. 127 (1975) 495.